Met O (APR) Turbulence and Diffusion Note No. 203

Empirical Diagnosis of Boundary Layer Depth

by

D R Middleton

27 August 1993

Headquarters, Bracknell

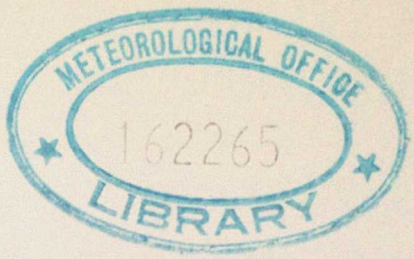

Met O (APR) Turbulence and Diffusion Note No. 203

Empirical Diagnosis of Boundary Layer Depth

by

D R Middleton

27 August 1993

Met O (APR)
(Atmospheric Processes Research)
Meteorological Office
London Road
Bracknell
Berks, RG12 2SZ

Note

This paper has not been published. Permission to quote from it should be obtained from the Assistant Director, Atmospheric Processes Research Division, Met O (APR), Meteorological Office, London Road, Bracknell, Berkshire, RG12 2SZ.

EMPIRICAL DIAGNOSIS OF BOUNDARY LAYER DEPTH

D R Middleton

27 August 1993

1 INTRODUCTION

The proper choice of boundary layer depth is a problem which has often vexed those who wish to calculate the spread of pollutants in the atmosphere. This report reviews ways in which that choice can be made and describes an empirical procedure that was developed as an option for the 'NAME' Nuclear Accident Model. Since the dispersion and deposition of radionuclides depend upon boundary layer depth, the work aimed to improve the diagnosis of this depth. Maryon and Best (1993) have compared estimates of boundary layer depth. The new empirical method can use temperatures and winds from the forecast or radiosonde ascents. It might be tested and improved using turbulence intensity profiles from field data. Symbols are defined at the end.

2 THE BOUNDARY LAYER

In a fluid whose viscosity is very small or Reynolds' number is very large:

'we should merely have the motion of frictionless fluid...were it not for the fact that fluid sticks to the boundary, a condition which cannot be fulfilled in the motion of frictionless fluid. Now closer investigation shows that though fluid with only slight friction behaves just like frictionless fluid at places where there is no boundary, a thin 'boundary layer' is formed at the walls as a result of friction, and that in this layer the value of the velocity varies from that corresponding to frictionless fluid motion to that involved by the fact that fluid adheres to the boundary. The smaller the viscosity, the thinner is this boundary layer. The frictional forces per unit volume are then very small in the interior of the fluid, whereas in the boundary layer they are of the same order of magnitude as the forces of inertia, as here, of course, the velocities are changed by finite amounts.' Prandtl (1952).

Batchelor (1967, page 302) defines a boundary layer in terms of vorticity:

'...a thin layer close to a solid boundary within which vorticity varies rapidly as a result of the combined effects of viscous diffusion and convection, and outside which the vorticity is zero (or is non-zero and varies only slowly)'.

He introduces

'the more general idea of a boundary layer, as being a thin layer in which the effect of viscosity is important however high the Reynolds number of the flow may be.'

2.1 Atmospheric Boundary Layers

Definition: Depth of the atmospheric boundary layer 'the height to which insignificant turbulent transfers of heat, mass and momentum between the local earth's surface and the atmosphere occur when averaged over a period of the order of an hour.' Arya (1981)

This height is important for a number of reasons (Arya, 1981):
1. It influences the mean flow and turbulence structure.
2. The dimensions of large eddies or roll vortices depend upon it.
3. Wind shears, turbulence intensities and fluxes depend on it.
4. Most dimensionless similarity formulations use it as an independent parameter.
5. It is required in several schemes parametrizing the boundary layer for large scale circulation models.
6. It is important in modelling atmospheric dispersion, often being called the mixing depth.

Scaling from Similarity The aim of similarity theory is to explain atmospheric field data. The formulation seeks to obtain results which might approach universal validity. According to Clarke(1970, page 93)...

'the analysis should be applicable, provided the assumptions are justified, to all parts of the turbulent boundary layer, including that near the ground'.

He points out that the similarity argument omits a number of possibly important factors such as horizontal non-uniformity, vertical velocity, radiative heat transfer, and time variability. A length scale based upon the ratio of friction velocity to Coriolis parameter, u_*/f, is implied, but other scales may be important. Clarke cites other possible scales, and reminds the reader that

'In equatorial regions f^{-1} as a time scale becomes meaningless, and here we might expect time and space variability of several quantities, such as temperature and velocity, as well as the' Monin Obukhov length L, 'to play a part in determining scales.'

In discussing scaling heights for the non-dimensional wind profiles, Clarke(1970,page 94) distinguishes unstable conditions from neutral and stable conditions. He suggests that an

unstable boundary layer extends to the inversion height z_i but there is also the Ekman scale z_E tending to produce some features in the profile related to $0.2u_*/f$, though z_i may be much larger than z_E. For neutral and stable conditions there is no counterpart to z_i, and the boundary layer may be presumed to coincide roughly with z_E. When we discuss recent work by Kitaigorodskii and by King (see below) we will see that u_*/N may be better than z_E in stable stratification.

We have therefore a generalisation by Clarke(1970) to the effect that, for unstable conditions, the boundary layer extends to the inversion height, whilst in neutral or stable conditions there may be no counterpart to inversion height (which depends on the history of the air-mass). In conclusion, diagnosis of the depth of the boundary layer must depend on whether conditions are stable or unstable. We now examine the unstable and stable cases in turn.

2.2 Unstable, convective conditions

In unstable conditions the height of the boundary layer usually coincides with the height of the base of the capping inversion. There are several ways of finding the height for the unstable case with an inversion above it. Arya (1981) reminds us that the capping inversion is a good indicator of boundary layer height in unstable conditions. Measurements of temperature taken at several heights (e.g. radiosonde, TV tower, or balloon cable) can be used to find the height of the inversion base. We shall see below that the new Sigma method is sensitive to an inversion above unstable conditions.

Remote Sensing by Sodar This remote sensing method relies on the backscatter of pulses of sound energy. The method has a limited vertical range, according to conditions. In monostatic mode, only the temperature inhomogeneities contribute to the backscatter, and entrainment causes a peak in signal at the height of the first inversion base, z_i. Melas(1990) said that 'sodar estimates of z_i are in very good agreement with rawinsonde measurements'. Although the sodars cited by Melas(1990) have a vertical range of 500-600m, he obtained values of z_i up to 2200m through the use of similarity profiles. Such an approach extends the range of measurement, but with increased uncertainty.

Enger (1990) describes an occasion when the 1600 m range of the sodar was less than the radiosonde mixing radiosonde depth at about 3000 m. Sodar echo signal was proportional to the temperature structure function whilst vertical standard deviation of velocity was obtained by the Doppler effect. Combining these gave an estimate between 2500 m and 3400 m. This indicates that sodar can be used in convective conditions to estimate mixing depths that are out of range (see Section 4 in Enger, 1990, for details).

Adiabat methods Radiosonde ascents may be analysed with a tephigram plot showing graphically the profiles of temperature and of dew point. The technique for identifying boundary layer depth appears to rely on judging where the temperature deviates from the adiabat, with the decision reinforced by looking for discontinuity in the dew point. Dew point often has a discontinuity above cloud. The author is of the opinion that this

approach is less well suited to automated processing than might at first be supposed. The discontinuities may be diffuse, or there may be more than one, so the diagnosis could be ambiguous.

Synoptic radiosonde ascents do not necessarily coincide with the times for which dispersion calculations are required. Holzworth (1974, 1972) obtained the morning and afternoon mixing depths using ascents recorded early in the morning. He assumed that surface temperature at the time of calculation can be extrapolated up a dry adiabat to meet the early morning profile at the mixing height. He assumed that the minimum (i.e. morning) temperature and the minimum mixing depth occur at the same time, and that the maximum (i.e. afternoon) temperature and the maximum mixing depth occur at their same time. For morning calculations the surface minimum temperature was increased by 5C to allow for heat island effects (Holzworth was interested in air pollution potential of urban areas but most radiosonde stations are at non-urban sites) and to ensure the start temperature of the adiabat was greater that the surface temperature reported by the sonde at the point of release. The use of a dry adiabat is due to the assumption of convective activity leading to a well mixed layer; his method can only be applied to unstable conditions. The method also assumes that there is no condensation, no precipitation, no convergence or divergence, and no temperature advection.

When radiosonde ascents coincide with the time of interest, Holzworth(1974) commended the method of Wuerch for midday ascents in which several criteria are tested in succession to locate the mixing height. This hierarchy of tests uses the following sequence:
inversion, isothermal, more stable than moist (i.e.pseudo-) adiabat, unlimited.
Each property is tested and the first to be found is taken to be an indicator of the mixing depth.

Holzworth(1974) points out that with an inversion at ground level the mixing depth by the adiabat method is zero, but this has no real meaning: his method is not applicable to the stable case. Note that the adiabat method (Method 6 in Maryon and Best, 1993) is akin to Holzworth's method.

2.3 Stable, nocturnal conditions

Stull (1988, page 15) describes how cooling at the ground transforms the lowest layer into a stable boundary layer. Whilst the wind approaches calm at the surface, winds aloft may accelerate to supergeostrophic speed, the 'low-level' or 'nocturnal' jet. Stability near the ground suppresses turbulence, while the developing jet causes wind shears that tend to enhance turbulence. The turbulence may occur in short bursts i.e. is intermittent. During non-turbulent periods, flow may be decoupled from the surface. In stable conditions, the measurement and calculation of boundary layer depth are therefore much more difficult and less reliable than in convection.

Wetzel (1982) discussed various methods which have been tried in earlier attempts to locate the depth of the stable boundary layer. He suggested that the diversity of methods is evidence that stable conditions present a problem. He cited:
1. The height where the stress is a small part of its surface value.

2. A scaling height u_*/f or $\sqrt{u_*L/f}$.
3. A bulk Richardson number.
4. The height of the low-level wind speed maximum.
5. The height of the maximum in the east-west component of the wind.
(This is unlikely to be of general application).
6. The height to which significant cooling extends.
7. The top of the surface temperature inversion.
8. The height of the lowest discontinuity in the temperature profile.

Wetzel (1982) suggested that in practice for stable layers, two definitions may be useful, depending on the problem:
1. The depth of the nocturnally cooled layer.
After studying field data, Wetzel proposed that there may be a statistical link between the depth of turbulence and the height to which the potential temperature increases linearly with height.
2. The height to which surface-linked turbulence extends.
The depth may also coincide with the point where wind velocity is a maximum (cf Mahrt et al., 1979). In stable conditions the depth may be diagnosed using zero wind shear or height of the jet. In the present work there were occasions when a low-level jet was absent from the stable profiles; the height of the jet is then an unreliable diagnostic.

The difficulties posed by the variability of the stable boundary layer were discussed by Derbyshire (1990). Physical processes such as waves, absorption of heat radiation near the top of the layer, drainage flows and other effects contribute to the unsteady nature of such boundary layers. Derbyshire extends the z-less scaling model of Nieuwstadt (1984) which postulated that vertical profiles of turbulence depend on the time history of the boundary layer ('z-less scaling' denotes a region where height is not important). Nieuwstadt solves the time dependent stable layer on the assumption of 'stationary' conditions i.e. that turbulent fluxes are not a function of time. Nieuwstadt's profiles agreed with carefully selected data from the mast at Cabauw, but he was careful to emphasise that they represent a special case, a slowly evolving stable layer. Derbyshire used numerical simulation to support his extension to the model and test the idea of steady conditions. These models provide valuable insights, but did not meet the requirement of diagnosis using NWP profiles as they rely on u_*/f.

Nieuwstadt (1984) chose data for stable conditions where:
1. They were well after transition (sunset) and before sunrise
2. The turbulence was continuous, not intermittent.
3. There were no gravity waves (which prevent the decrease of turbulence with height).
In those data where the depth seen on the sodar was below the height of the mast, the turbulence intensity above the stable boundary layer was negligible. The boundary conditions in Nieuwstadt's model include the condition that turbulence vanishes at the top of the boundary layer. This is a similar if stricter condition than our criterion that the boundary layer depth is diagnosed where $\Sigma \leq \Sigma_0$ (see section 4.1 below).

Remote Sensing by Sodar Cheung(1991) has studied the atmosphere in stable conditions at Barrow, Alaska by means of sodar and other instrumentation. The observations included gravity waves and low level or ground based inversion layers. Multiple inversions

were also seen. Thin surface based inversions with heights less than 150m were often seen, and overlying inversions were below 1.5km. Cheung (1991) discussed a climatological summary of inversion bases produced by Kahl: for March and April the monthly median height of inversion bases was 57m to 133m, with inversion depths 700m to 850m.

Koracin and Berkowicz(1988) studied stable nocturnal boundary layers using two sodars operated 15km apart; the data from the two instruments were similar. They discussed several formulae for boundary layer depth. However no evidence was found to support the Zilitinkevich (1972) formula for stable conditions, $c\sqrt{u_* L/f}$ with c in the range 0.22 to 0.7. The most significant point was the experimental observation that boundary layer depth in stable conditions was directly proportional to the friction velocity.

Arya (1981) says that sodar or lidar provide the only reliable means of measuring the height of the stable boundary layer. However other workers have emphasised the value of turbulence measurements, e.g.bivanes(as discussed next), for finding the depth of the nocturnal boundary layer.

Wind and Temperature Measurements The nocturnal boundary layer was studied by Kurzeja et al. (1991). They recorded several meteorological parameters on a 300 metre tower. The difficulties in diagnosing boundary layer depth even from good field data are discussed in this paper. Methods based on mean profiles are poorly correlated with one another. This may be due to radiative cooling so that the inversion is deeper than the turbulent layer. Thus Mahrt et al. (1979) discuss the increase with time of the inversion layer due to radiation cooling, whilst the turbulent layer and jet level may be constant or decrease with time. The top of the turbulent layer seems to occur just below the low level wind maximum, but the inversion depth can be about 1.25 times the jet level. Kurzeja et al. (1991) said that 'it is preferable to use actual measurements of turbulence', rather than 'the gradient of mean variables such as temperature, wind speed, or Richardson Number' to estimate the nocturnal planetary boundary layer depth. In other words, field measurements of turbulence are the preferred method. This was an important consideration in the present work whose aim was to improve a model that relied upon Richardson number for its boundary layer depth. Kurzeja et al. (1991) measured the turbulence by the standard deviation of azimuth angle (after filtering). Nocturnal boundary layer depth was determined from this measure. The use of wind fluctuations is considered again in Section 3.3.

Kitaigorodskii scaling in stable stratification Kitaigorodskii (1988) and Kitaigorodskii and Joffre (1988) discussed the failure of the Ekman boundary layer model in the presence of imposed stable stratification; such failure is because the stratification can prevent the depth reaching the neutral Ekman length scale of u_*/f. Kitaigorodskii introduces a scaling length of u_*/N to which boundary layer depth is directly proportional. If the Brunt Vaisala frequency N is constant, the result of Kitaigorodskii reduces to boundary layer depth being proportional to friction velocity, as observed by Koracin and Berkowicz (1988).

Kitaigorodskii (1988) emphasises (p 438) that in the presence of imposed stable stratification, rotation is probably not important. This would rule out the Zilitinkevich formula

in many situations and is therefore consistent with the work of Koracin and Berkowicz cited above.

Formulae involving u_*/f will clearly break down at the equator (f=0), but have often been used at higher latitudes. In this context the measurements reported by King(1990) are of interest; the site is at high latitude (75 36 S, 26 40 W) at Halley in the Antarctic, and conditions varied from near-neutral to stable. The neutral boundary layer depth was much smaller than expected and it did not scale according to u_*/f. King suggests that the presence of stable stratification limits the depth of what seems to be a neutral boundary layer. This situation is thus reminiscent of that considered by Kitaigorodskii (above), although futher data are needed to see if the u_*/N scaling applies.

2.4 Calculation from surface observations

Surface observations are used by The Meteorological Office in supplying frequencies of Pasquill categories and mixing depths to clients. Boundary layer depth is calculated from the friction velocity and the sensible heat flux (which must be integrated from dawn). The heat flux is estimated from routine surface observations and is based upon the Penman-Monteith model. The friction velocity is initialised to a neutral value using wind speed. Iteration is applied to improve the solution. This algorithm can only be used at certain sites where the raw data are measured enough times during the day to minimise the errors. The equations are in Farmer (1984).

2.5 Saturation Point method of Betts

Several thermodynamic variables can be calculated from the radiosonde data, Betts(1982a, 1982b). Pressure, temperature and dew-point can be used to calculate the saturation-point pressure P_{SL} and temperature T_{SL}. Then θ_{SL}, the potential temperature using T_{SL} and P_{SL}, is found. These are used to obtain three quantities:
1. Pressure difference $\mathcal{P}$, the saturation point pressure minus the pressure of the air parcel in its original state, $P_{SL} - P$.
2. Equivalent potential temperature
$\theta_E \approx \theta exp(\lambda r/C_pT) \approx \theta(1 + \lambda r/C_pT)$
3. Saturation point equivalent potential temperature
$\theta_{ES} \approx \theta_{SL} exp(\lambda r_{SL}/C_pT_{SL}) \approx \theta_{SL}(1 + \lambda r_{SL}/C_pT_{SL})$
Other symbols are listed separately.

Betts and Albrecht(1987) pages 91-2 observed that the minima in both θ_E and $\mathcal{P}$ and the maximum in θ_{ES}, all coincided with the top of the convective boundary layer (within $\pm$ 10 hPa). Parasnis and Morwal (1991) used the minima in θ_E and $\mathcal{P}$ to locate the top of the convective boundary layer. This approach seems particularly appropriate for tropical convection with high humidity. We postulate that the difference $\theta_{ES} - \theta_E$ may exhibit a well defined and unambiguous maximum at the top of the boundary layer because it is the difference between terms which go to a maximum and a minimum; such a maximum might be readily found in an automated procedure. How it would perform as a diagnostic

for boundary layer depth when applied to non-convective situations is unclear and would need investigation.

3 SPECIFICATION OF NEW METHOD

3.1 Background

It is possible to use a critical value of Richardson number in order to locate the top of the boundary layer. However given that methods based upon Richardson number are flawed by discontinuities which appear when using a layered representation of the atmosphere, another approach was deemed desirable. The aim of this work was to seek a method that could apply to data from forecast or actual ascents. The data are restricted in scope to those variables passed to 'NAME'.

The idea was to define some measure which relates to the effectiveness of the atmosphere in causing mixing (dispersion) and which does not change sign with stability. A well defined criterion for the height of effective mixing might then be specified using some critical value of this measure. Also, if the measure relates directly to mixing it should be possible to compare it with values derived from field observations. The measure should be a continuous function of height, falling to a small value outside the boundary layer where mixing is small. It should remain finite, since there are practical limits to mixing. The measure should keep the same sign in neutral, stable or convective conditions. The measure should be calculable from the variables that are available from the forecast model and give answers that can be compared with measurements in the field. It should be such that analysis of its variation with height can give an unambiguous result for the mixing depth. Thus was the goal defined.

3.2 Possible approaches

In terms of air pollution modelling the requirement is to identify some height above which the rate of mixing is significantly less than that near the ground. Four approaches were identified:

1. An inversion layer where potential temperature increases with height will suppress vertical transport of pollutants and is, in effect, a 'lid' on urban pollutants. The height of the inversion can be found from the variation of potential temperature with height, but it is necessary to define in an arbitrary manner the value of $\frac{\partial \theta}{\partial z}$ at which inversion is detected. The adiabat method of Holzworth (above) can be used in unstable conditions. The procedure must cope with the possibility of more than one inversion. Mixing also occurs due to turbulence caused by drag at the ground, but temperature profiles convey no information about the wind shear. Finding the height(s) of inversion layer(s) may be necessary but is not sufficient to determine boundary layer depth in all situations.

2. The Richardson number Ri is a measure of the balance between the rate of creation of

turbulence kinetic energy by mechanical action (wind shear) and the rate of suppression of turbulence kinetic energy by the buoyancy force associated with the temperature stratification. Although Ri is uniquely defined in terms of the potential temperature gradient, wind shear etc, it is not proportional to mixing effectiveness because it changes sign, even when turbulent mixing may still be present.

3. The eddy diffusivity K (−flux of pollutant divided by the pollutant gradient) is a measure of the rate of diffusion which depends on the turbulence in the flow. It does not depend on the molecular diffusion. K might seem to be ideal for diagnosing the mixing depth but there are two disadvantages. The definition of K assumes that the process is Fickian; this may not be valid. There is also the practical limitation that vertical profiles of K are not easily measured; experimental validation of the depths derived from profiles of K will be difficult.

4. Mixing in the atmosphere depends upon turbulent eddies, so the desired measure should relate to this aspect of the flow. The movement of the air is thus crucial to the defining of a measure from which boundary layer depth or mixing depth is to be found. The available candidates include fluctuations of wind direction, measures of crosswind and vertical displacements of particles, or fluctuations of velocity components. Any of these can be measured in the atmosphere and used to test model results.

3.3 Wind fluctuations

There are three types of interrelated parameter to describe wind fluctuations, but to be useful for the present problem they would have to be calculable from forecast profiles. They are as follows:

1. The standard deviations of crosswind and vertical displacement of particles (σ_y, σ_z) which have long been used in gaussian plume models for air pollution. They depend upon the downwind distance (or travel time) and stability i.e. according to the turbulence.

2. The standard deviations of wind direction components (σ_θ, σ_ϕ) which measure the fluctuations of wind direction. They increase in magnitude as the air becomes more turbulent, being larger in convective conditions and less in stable ones, Hanna et al.(1982), p 28. These parameters are often measured in air pollution field surveys, because the necessary instrumentation (e.g. bivane) is reasonably economical and the results relate to the turbulent mixing. Kurzeja et al. (1991) used bivane data to locate the boundary layer depth (above). This procedure could be tried were it possible to calculate profiles of σ_θ.

3. The standard deviations of wind-velocity components (σ_u, σ_v, σ_w) which describe the turbulence of the flow. When normalised with respect to the mean wind-speed u they give the components of turbulence intensity. The intensities σ_u/u and σ_v/u decrease with height for all stabilities, whereas σ_w/u increases with height in unstable conditions and decreases with height in neutral and stable conditions (Hanna et al. (1982), pages 7-8). Testing vertical profiles of the turbulence seems to be the ideal method of determining boundary layer depth (see Section 4).

Statistics such as the standard deviation of the fluctuations of the wind velocity component depend upon the averaging time. Unambiguous definition of boundary layer depth using these statistics or other methods requires the averaging time to be specified. This is often done implicitly.

3.4 Summary of criteria

To summarise the above criteria, the desired procedure to diagnose boundary layer depth should employ a variable which has the following properties:

1. Depends upon wind fluctuations
2. Increases as the turbulent mixing increases but remains finite
3. Will always be greater than or equal to zero
4. Is able to be calculated from forecast suite output
5. Is able to be calculated from measured quantities in the field
6. Depends upon averaging time
7. Will be amenable to experimental testing
8. Leads to an unambiguous diagnosis of the depth in any conditions.

4 THE SIGMA METHOD

4.1 Outline

The method that is now to be described is empirical in the sense that it began with some field measurements reported by Bultynck and Malet (1972), but has been adapted and evolved to try to get it to fit as wide a range of radiosonde ascents and model profiles as possible. The method has been given the acronym 'Sigma' simply because it is also related to the standard deviations σ_y and σ_z that are familiar in gaussian plume models of atmospheric dispersion.

The method looks for a height above which the rate of mixing becomes small. Two papers cited below describe a stability parameter S that can be calculated from the forecast suite variables available within 'NAME'. S can be used to obtain a measure which obeys many of the above criteria. Benaire (1980) describes the Bultynck-Malet stability parameter S, which uses just wind velocity and potential temperature gradient. Bultynck and Malet (1972) present empirical formulae whereby their S-parameter can be used to calculate the gaussian plume parameters σ_y and σ_z for a given travel distance x in the downwind direction. In the empirical Sigma method we calculate the dimensionless quantity

$$\Sigma = \frac{\sqrt{\sigma_y \sigma_z}}{x} \qquad (1)$$

Σ increases from zero as mixing increases, and is never negative. It can be obtained from field measurements of wind fluctuations, or calculated indirectly from stability parameters such as S using readily available parameters. Modelling and experiment can then

be compared (in principle) to verify the variation of Σ as a function of the height z. A critical value Σ_0 is proposed as the criterion defining where the boundary layer or mixing depth should be set. In the light of applying early versions of the Sigma method to a number of profiles, some additional adjustments have been incorporated into the method (see below), but the above outlines the general idea.

In the next section a more fundamental definition of Σ will be given, together with the derivation of the above form. Then an empirical method of estimating Σ is described

4.2 Derivation of Sigma, Σ

In the notation of Bultynck and Malet (1972), the instantaneous wind components are u, v, w aligned parallel and orthogonal to the mean wind. The mean is denoted by an overscore, with deviations from the mean denoted by a prime. These components are Eulerian measures of the wind taken on a mast.

$$u = \overline{u} + u' \tag{2}$$

$$v = v' \tag{3}$$

$$w = w' \tag{4}$$

Turbulence statistics depend on the averaging time T which is used in the calculations of the running means. In order to choose a suitable averaging time it must be recognised that the anemometer is fixed upon a mast, giving an Eulerian measure of the turbulence. However the mixing of a pollutant is a Lagrangian process as the admixture is borne along with the mean wind-speed. The averaging times are found as follows after Hay and Pasquill (1959, p 351) who defined their β as the ratio of the Lagrangian to Eulerian time scales; equations 7, 8 below were given by Wandel and Kofoed-Hansen (1962) and used by Bultynck and Malet (1972):

$$T_y = \frac{x}{\beta_y \overline{u}} \tag{5}$$

$$T_z = \frac{x}{\beta_z \overline{u}} \tag{6}$$

where x is the distance travelled with the wind at mean wind speed $\overline{u}$ in the travel time $\frac{x}{\overline{u}}$.

Also, β_y and βz depend upon the Lagrangian and Eulerian time scales of turbulence:

$$\beta_y = \frac{\sqrt{\pi}}{4} \overline{u} (\overline{v'^2})^{-\frac{1}{2}} \tag{7}$$

$$\beta_z = \frac{\sqrt{\pi}}{4} \overline{u} (\overline{w'^2})^{-\frac{1}{2}} \tag{8}$$

For a sampling interval B (say 3600 s), with the above averaging time T_y or T_z, the crosswind and vertical standard deviations of a point source plume are related to the turbulence by:

$$\frac{\sigma_y(x)}{x} = \overline{\left[v'^{\,2}_{x/(\beta_y \overline{u})} \right]}_B^{\frac{1}{2}} / \overline{u} \tag{9}$$

and

$$\frac{\sigma_z(x)}{x} = \overline{\left[w'^2_{x/(\beta_z\overline{u})}\right]_B}^{\frac{1}{2}}/\overline{u} \tag{10}$$

The above notation is given in Appendix 1.

Turbulence in the horizontal or vertical can cause mixing, so combining these measures by geometric mean yields the two forms:

$$\Sigma = \sqrt{\overline{\left[v'^2_{x/(\beta_y\overline{u})}\right]_B}^{\frac{1}{2}}\overline{\left[w'^2_{x/(\beta_z\overline{u})}\right]_B}^{\frac{1}{2}}}/\overline{u} \tag{11}$$

and

$$\Sigma = \sqrt{\sigma_y(x)\sigma_z(x)}/x \tag{12}$$

Equation 11 can be used to find Σ from the fluctuations of the components of wind velocity. These velocities could be measured in the field or taken from numerical simulations of turbulence. Equation 12 allows Σ to be estimated from the spread of particles as described by the point source plume spread parameters at various heights for different stabilities. These parameters can be estimated via equations 9, 10. Their behaviour may diverge in the stable boundary layer, but even so if one of them tends to zero above the boundary layer, then so will Σ in equation 12. Field measurements of the wind components u, v, w can be used to assess the dependence of equation 11 on height and averaging time. The latter may be of significance in stable boundary layers whose stationarity is uncertain.

Σ is a measure of the efficiency of mixing by turbulence. It depends upon how much a plume will spread crosswind and vertically relative to its travel distance. Σ is positive, increases as turbulence increases and depends upon the averaging time. It is likely that Σ will decrease with height because of decreasing effects of surface roughness and because a stable temperature gradient is likely to be met. This implies that the height where Σ obeys a suitable test can be diagnosed as the boundary layer depth. The test is discussed in a later section. Σ has the important property that it is amenable to experimental study.

4.3 Depth Criterion

In order to use Σ to diagnose boundary layer depth a suitable criterion must be chosen. It must be well behaved in all conditions, not leading to absurd heights. It must reflect pronounced discontinuities in the profiles, such as strong inversions. Several criteria are possible but after some trials it was decided that the simplest method was the best. The required depth becomes the height where Σ first falls to less than a value Σ_0. The testing starts from just above the ground to avoid surface effects (at the surface in 'NAME', the wind speed is zero)

Two special cases can arise:
1. In very strong winds, Σ should be quite large near to the ground, but decrease rapidly when the shear is less
2. With nocturnal surface inversions, the air near the ground may be very still, and Σ may not even reach the threshold of Σ_0

4.4 Value of the Threshold

The threshold value Σ_0 represents the idea that at points above the boundary layer there is less turbulent mixing. If Σ_0 is too large, very shallow boundary layers are diagnosed. If it is too small, the depth may be diagnosed as too deep. Clear air turbulence or wave motions above the boundary layer might cause $\Sigma > \Sigma_0$ but are not considered here. The choice of Σ_0 will now be discussed.

Bultynck and Malet (1972) gave empirical curves for $\sigma_y(x)$ and $\sigma_z(x)$. The boundary layer top is to be the height where conditions are most stable. In defining the threshold Σ_0 we need to know how the dimensionless quantity $\Sigma(x)$ varies with x.

For the stable category denoted E_1, Bultynck and Malet (1972) give the following:

$$\sigma_y(x) = 0.235x^{0.796} \tag{13}$$

and

$$\sigma_z(x) = 0.311x^{0.711} \tag{14}$$

From equations 12,13,14 we found that for x between 100 m and 18 km, $\Sigma(x)$ varied from 0.087 to 0.024. Beyond 1km the value of $\Sigma(x)$ in stabilility E_1 did not change very much. It was therefore decided to round the 1 km value of $\Sigma(x) = 0.0493$ to 0.05. In the present work, the threshold was defined using the minimum value of Σ for each profile, but not less than 0.06. Then

$$\Sigma_0 = \Sigma_{min} + 0.01 \tag{15}$$

If $\Sigma_0 < 0.06$ then $\Sigma_0 = 0.06$.
This procedure was adopted to ensure that the method was able to cope with a wide variety of model profiles.

4.5 Empirical Sigma Method: Σ From Profiles

In the present context it was desirable to estimate Σ from model products as will now be described. The first step is to obtain the stability.

The Monin Obukhov length requires the measurement of friction velocity and vertical heat flux 'which are not easy to obtain in current practice' while the Richardson number has the square of vertical shear in the denominator, but this is 'also difficult to measure with the required accuracy'. Bultynck and Malet (1972) therefore adopted the parameter S to characterise the stability:

$$S = \frac{\partial\theta}{\partial z} / \overline{u}_{69}^2 \tag{16}$$

where $\frac{\partial\theta}{\partial z}$ is the vertical gradient of mean potential temperature in the layer from 8 m to 114 m and $\overline{u}_{69}$ is the mean wind speed at the height of 69 m. They state that 'studies of the wind profiles between 2 and 120 m have shown that the parameter S is unequivocally bound to the Monin-Obukhov length L.'

The parameter S has three advantages:

1. It uses just the potential temperature, wind speed and height
2. It can be used to obtain $\sigma_y(x)$ and $\sigma_z(x)$ at x, from which we estimate $\Sigma(x)$. As in the above section, we used $x = 1km$.
3. It can be calculated using forecast or actual ascents.

Bultynck and Malet (1972) selected data from meteorological measurements taken at Mol in Belgium. They applied strict criteria before using the data in curve-fitting for the stable ($S > 0$) or unstable ($S < 0$) cases. The general curve used for σ_y or σ_z was as follows:

$$\sigma(x, |S|) = \sigma(x, 0) \left[\frac{b + c|S|10^6}{b + |S|10^6} \right] \tag{17}$$

where $\sigma(x, 0)$, b, c were constants, values of which were determined from the data for downwind distances of 100 m, 500 m, 1000 m, 5000 m, 10000 m. Note that b and c also depend on the sign of S.

In order to estimate Σ, formulae were chosen according to the magnitude and sign of S i.e. according to stability:
Neutral $S = 0$

$$\sigma_y(1000, 0) = 100 \tag{18}$$

$$\sigma_z(1000, 0) = 73 \tag{19}$$

Stable $S > 0$

$$\sigma_y(1000, |S|) = 100 \left[\frac{60 + 0.57|S|10^6}{60 + |S|10^6} \right] \tag{20}$$

$$\sigma_z(1000, |S|) = 73 \left[\frac{158 + 0.52|S|10^6}{158 + |S|10^6} \right] \tag{21}$$

Unstable $S < 0$

$$\sigma_y(1000, |S|) = 100 \left[\frac{510 + 2.5|S|10^6}{510 + |S|10^6} \right] \tag{22}$$

$$\sigma_z(1000, |S|) = 73 \left[\frac{2480 + 3.63|S|10^6}{2480 + |S|10^6} \right] \tag{23}$$

Thus for a downwind distance of 1000 m, values for σ_y and for σ_z in metres were obtained and used to calculate Σ.

Radiosonde profiles Temperatures and winds may be reported at different pressures, so must be processed separately. The potential temperature and windspeed at a series of heights are calculated. S is found using the gradient of potential temperature across the layer, with the wind speed at each height. Given S, Σ for $x = 1000$ m is calculated and tested to see if it has fallen to less than Σ_0. When it does so, the procedure has found the desired depth and processing halts.

'NAME' model profiles The forecast or analysed products held on a special archive can be read by the 'NAME' model. Temperatures, windspeeds and directions are available at several levels and at each grid point. Potential temperature and the height of each level are calculated. S, σ_y, σ_z, and Σ are calculated as above. The desired depth is found by testing Σ and processing halts.

4.6 Extrapolation of S

The work of Bultynck and Malet (1972) was for a height of 69 m, and it has been necessary to extrapolate up to 5000 m. The wind speed should be adjusted allowing for the diminishing effects of the ground at greater heights. The profile should change with the stability conditions. However the following adjustment has been adopted:
For $z > 69$ m,

$$u_{69} = u_z \left(\frac{69}{z}\right)^m \tag{24}$$

with exponent m=0.5 for any stability. Thus in Equation 16, the exponent m=0.5 increases $|S|$ in proportion to $z/69$. An adjustment based upon the wind shear was tested, but did not seem any better than the above.

Cieslek et al.(1981, page 373) studied the exponent m on a tower for wind-speeds recorded at heights of 24 m and 69 m. Shortly after sunrise m ranged from 0.6 to 1.0, whilst in the early afternoon it was near 0.0. Their Figure 3 plots m against time of day for August 1-2, 1977 on a scale 0 to 1; a line drawn at m=0.5 (used in the present work) divides the data in two. For this height range the value seems reasonable but at greater height its validity is uncertain. In their Figure 3, m depends on lapse rate according to an approximate relation (M Best, personal communication)

$$m = \frac{\log\left(100\frac{\partial\theta}{\partial z} + 2\right)}{log(7)}$$

In this form, for unstable conditions m tends to zero and the adjustment factor $(69/z)^m$ tends to unity: the influence of z is reduced. This was tried in a few cases and had a small effect on the diagnosed depth.

In summary, the diagnosis is less sensitive to wind-speed profiles than to gradient of potential temperature. The sensitivity of the empirical Sigma method to wind adjustments has not been quantified (apart from the above study of m). A study of measured turbulence intensity profiles may lead to a better approach, because Sigma can be directly related to turbulence intensity. This could be an area for fruitful research.

4.7 Neutral Conditions

Tests revealed that it was advisable to broaden the range of neutral conditions to a wider range of values than implied by the identity $S = 0$. Once the gradient of potential temperature has been calculated, gradients in the interval $\pm$0.5 K/km are set to zero and cause $S = 0$. A range of values on S is also defined so that the three cases become:
1. Stable $S > 6.324556 \times 10^{-5}$
2. Unstable $S < 6.324556 \times 10^{-5}$
3. Neutral $|S| < 6.324556 \times 10^{-5}$

The adjustment to the gradient is analogous to an observer taking a slight slope on the adiabat as defining the extent of neutral stability. The limits on S extend the neutral case to larger $|S|$ than just zero (i.e. to $\lambda = 1.8$ in Figure 1-2 of Bultynck and Malet (1972)). Tests were conducted whereby a gradient of 0.00098 K/m (one-tenth of the dry adiabat)

was subtracted from $\frac{\partial\theta}{\partial z}$ (i.e. replacing the above interval); it gave modest increases in the depth in some cases. Section 5.2 also considers the effect of the strength of the inversion when diagnosing its depth.

4.8 Stable Conditions

In stable conditions with a strong surface inversion the Sigma method detects the positive $\frac{\partial\theta}{\partial z}$ and returns a minimum height. Mahrt et al.(1979) discussed the use of the nocturnal jet as an indicator of the depth of the stable boundary layer. When included in the code, this worked for a number of midnight ascents, giving more realistic depths than Sigma had. However when tested on forecast profiles the results were disappointing because the wind profile sometimes had a maximum at great height (even reaching the highest level in 'NAME' on occasion, which is clearly too high).

4.9 Windspeeds

Windspeed was reset to 0.2 m/s if it was ever less than this figure.

When windspeeds exceeded 11.5 m/s and the wind shear exceeded 0.1667 /s, then the special category E_7 of Bultynck and Malet (1972) for strong winds was applied:

$$\sigma_y = 1.043x^{0.698} \tag{25}$$

$$\sigma_y = 0.819x^{0.669} \tag{26}$$

The testing of shear is not in the original specification of category E_7, but was included after plotting some profiles with a very pronounced shear near the ground and high wind speed. Some profiles over the sea had shown that without the testing of shear, the Sigma method was missing a pronounced change in the wind profile when the wind increased rapidly with height and then was nearly constant with height.

4.10 Extreme Conditions

In Equation 17 as $|S|$ increases, $\sigma(x,|S|)$ tends to a constant value $\sigma(x,0)[c]$. This means that in very stable or very unstable conditions the dependence of σ_y and σ_z on $|S|$ will diminish and Σ also tends to a limit. The following forms were tried:
Stable $S > 0$

$$\sigma(x,|S|) = \sigma(x,0)\left[\frac{b + c|S|10^6}{b + |S|10^6 + d|S|^2 10^{12}}\right]$$

Unstable $S < 0$

$$\sigma(x,|S|) = \sigma(x,0)\left[\frac{b + c|S|10^6 + d|S|^2 10^{12}}{b + |S|10^6}\right]$$

With d=0.000020, Σ showed a small variation with $|S|$ in strongly stable or unstable conditions. The profiles of Σ were changed slightly in magnitude and slope but in most of the (few) profiles tested, the diagnosed depth was little changed.

5 RESULTS

The results of the Sigma method are best demonstrated by typical profiles which compare the model profiles with radiosonde ascents. A small sample of the many possible profiles for midnight and midday appear in Appendix 2. Each page refers to radiosonde measurements or to 'NAME' model profiles (the latter from the forecast suite) and are labelled accordingly. The date and time are given. Positions are identified by the name of the relevant radiosonde station. The grid point is for the Limited Area Grid and some points are just off the coast from the adjacent radiosonde station. Since these stations are all within 5 degrees of the Greenwich meridian, the profiles can be regarded as being at the same solar time.

Each figure contains four profiles, with height calculated from the hydrostatic equation (applied to each layer in turn). The four profiles are as below:
1. Dew point and temperature
2. Wind-speed
3. Potential temperature.
4. The empirical Sigma parameter Σ.

Equations 12, 16-23 were used to estimate Σ as a function of height from the values of potential temperature and wind-speed interpolated at each step. A broken line is drawn at the height where Σ crosses the threshold Σ_0 and indicates the boundary layer depth as diagnosed by the empirical Sigma method. This height should be compared with the profiles 1, 2 and 3.
In a number of cases, the actual and model profiles agreed sufficiently for them to give similar diagnosed depths. In other cases the profiles and depth results were quite different. It is worth noting that the actual ascents show dew point, but this information is not used in the Sigma method. The reader will find the dew point is useful when studying the curves. The depth is diagnosed in actual or model profiles using the same Sigma algorithm. Wind data for radiosonde ascents are archived at different heights to the temperature measurements, so interpolation was used to find temperature and wind speed at each step height.

5.1 Profiles for midnight

Many show stable conditions with a surface inversion, but some are sensitive to the wind speed. This is because the Sigma method is affected by wind speed as well as potential temperature gradient. Lerwick had strong wind speeds and demonstrate that the method responded to the wind speed as well as to the temperature profile.

CRAWLEY 13 August 1991 Midnight This is an inland site, and the 'NAME' grid-point is 16860. This radiosonde profile was at a time when pressure was high and winds were light. As expected it shows marked surface cooling by long-wave radiation during the night. The surface inversion is well developed. The Sigma method diagnosed a minimum depth (65 m), reflecting the dominance of the stable gradient of potential

temperature at the surface. The empirical Sigma method often returns a minimum depth in stable conditions because the method responds more to potential temperature gradient than to wind-speed. The profile is a classic case of shallow depth in light wind and surface inversion.

LERWICK 18 April 1993 Midnight This is a coastal site in Shetland, and the 'NAME' grid-point is 12502. The wind-speed was above 15 m s^{-1} and the potential temperature gradient was stable. The strong wind meant that Σ was large up to 2 km; 'NAME' (1940 m) and radiosonde profiles (2129 m) both show Σ_0 was reached near this height. A deep boundary layer is diagnosed in either case.

TRAPPES 18 April 1993 Midnight At this site, the wind speed was not quite so high and the gradient of potential temperature was more stable. This is an inland site near Paris, and the 'NAME' grid-point is 17781. The model and radiosonde depths were diagnosed to be shallow and different. The 'NAME' data for potential temperature at Trappes has a slightly less stable region near the ground and a deeper layer is diagnosed (247 m). The stable radiosonde profile yields a shallower depth (139 m).

5.2 Profiles for midday

At midday the well mixed layer may be characterised by a high surface temperature with an inversion aloft. The well mixed layer is most easily seen in the potential temperature profile. The Sigma method often returns a depth that is representative of temperature inversion. Sometimes the result seems low, because it has detected the first sign of inversion, and not reached a higher level where the inversion may be much stronger. This is an important point, for it may be desirable in future to increase the gradient $\frac{\partial\theta}{\partial z}$ to diagnose the stronger inversion (cf Section 4.7 above). The midday profile of potential temperature at Crawley (13/08/91) is an example, as now follows.

CRAWLEY 13 August 1991 Midday This is an inland site, and the 'NAME' grid-point is 16860. Pressure was high and the wind-speed was low. The surface temperature is raised due to solar heating. The potential temperature shows convection reaching 1100 m. The diagnosed depth (811 m) is less than this because the method has detected the first signs of inversion; a stronger inversion is seen in the radiosonde profile at 1100m. The Sigma values are smaller above the inversion, except at 2300-2500 m where the change in lapse rate has suggested an increased turbulence in this layer. This layer stops at the subsidence inversion shown by the dew-point.

HEMSBY 18 April 1993 Midday Hemsby is a coastal site and the 'NAME' grid-point was 15946. The diagnosed depths were similar for the radiosonde and model profiles. The radiosonde ascent has surface potential temperature very slightly greater than the air above it. The depth is diagnosed at 922 m. In the 'NAME' profile for potential

temperature the surface value is low because the grid-point is just off the coast and the sea is cooler than the air above it. However the method still diagnoses the unstable layer and finds the depth at 980 m. Both diagnoses are noticeably above the inversion at 700 m; they reflect the influence of wind-speed.

NIMES 18 April 1993 Midday Nimes is an inland site, with 'NAME' grid-point 19850. Depths disagree because the model (1238 m) and radiosonde (1599 m) profiles differ. The radiosonde shows a classic unstable boundary layer with hot surface; 'NAME' has a similar but shallower structure. In both cases the depths are placed at the inversion.

5.3 Summary of Profiles

The radiosonde profiles for Crawley on 13/8/1991 at midnight and midday are classic examples of the two cases: overnight inversion and daytime convection. As discussed elsewhere the stable conditions in the inversion are difficult to handle and the empirical Sigma diagnosis is usually the minimum depth. Stable conditions merit the greatest attention in future studies. Other profiles also illustrated the effect of strong winds.

6 CONCLUSIONS

1. This work hypothesises that the geometric mean turbulence intensity Σ as defined by equation 11, meets the criteria for unambiguous diagnosis of boundary layer depth. It depends directly upon wind fluctuations, increases with the turbulence, remains positive (but can be zero) in all stabilities, and depends (probably weakly) upon averaging time. It is further hypothesised that Σ can be tested against a criterion Σ_0 to diagnose the depth. Σ can be measured in field trials using wind fluctuations for a fixed averaging time.

2. An empirical Sigma method was developed from Equation 12 to estimate the boundary layer depth from radiosonde ascents and forecast profiles. It uses potential temperature and windspeed at a series of heights to find values of a stability parameter S. It is however necessary to extrapolate the empirical curves (see Equations 16-23) of σ_y and σ_z versus S to the required heights. There is scope to adjust the method to the desired strength of inversion.

3. The empirical method worked quite well in unstable or neutral conditions. Potential temperature plotted against height often exhibits a pronounced discontinuity at the inversion. There is then relatively little difficulty in judging by inspection whether the Sigma method has responded to the presence of the inversion. The method usually returns shallow depths in stable conditions, at or only just above the initial height from which the algorithm begins its search.

4. The empirical approach has been found very robust: it rarely seems to give absurd diagnoses such as very deep layers. This is important if the method is to be used at any

grid point in 'NAME' at any time.

5. The empirical method recognises that mechanical and thermal processes cause turbulence; the method is sensitive to both the windspeed and potential temperature. However considerable uncertainty surrounds the extrapolation to reach greater heights, so more work here would be advisable. Radiosonde ascents can validate the depth when discontinuities are pronounced, but this is not always so. Lack of clear guidance from some measured profiles hinders the validation of algorithms for boundary layer depth; other data (such as sodar, lidar, or turbulence probes on balloons or aircraft) are thus desirable. In this regard, measurements of turbulence intensity would be of most value to improve the method.

6. It is proposed that field data be used to plot Σ (Equation 11) as a function of height and stability. The data should range from near the ground to well above the top of the boundary layer. The three- dimensional geometric mean of all three turbulence intensity components might also be studied. Such a study might test the hypothesis that Σ can be used to diagnose boundary layer depth.

7. Maryon and Best (1993) have also examined boundary layer depths using six different methods. They employed a sample of radiosonde ascents as reference data.

8. Field validation of methods for diagnosing boundary layer depth could enhance the simulation of radionuclide behaviour in the atmosphere.

7 SYMBOLS

b	Constant
B	Sampling time
c	Constant
d	Constant
C_p	Specific heat at constant pressure for dry air
E_1	Stable stability class
E_7	Strong wind stability class
f	Coriolis parameter
K	Eddy diffusivity, or Kelvin
L	Monin Obukhov length
m	Exponent in wind profile, Equation 24
N	Brunt Vaisala frequency
P	Pressure of air parcel
P_{SL}	Pressure of air parcel expanded adiabatically to saturation level
r	Humidity mixing ratio
r_{SL}	Humidity mixing ratio for parcel at its saturation level
Ri	Richardson number
S	Stability parameter
T	Averaging time for running mean
T_{SL}	Temperature of parcel expanded adiabatically to saturation level
T_y	Averaging time for running mean of y component
T_z	Averaging time for running mean of z component
u	Wind velocity component in direction of mean wind
u_*	Friction velocity
u_z	Wind speed at height z
u_{69}	Wind speed at 69 metres
v	Wind velocity component orthogonal to mean wind
w	Wind velocity component in the vertical
x	Distance downwind from plume release
y	Distance crosswind from plume centre-line
z	Distance vertically from plume centre-line, also height
z_E	Ekman layer height
z_i	Inversion height
β	Ratio of the Lagrangian to Eulerian timescales
β_y	Ratio of the Lagrangian to Eulerian timescales for component v
β_z	Ratio of the Lagrangian to Eulerian timescales for component w
θ	Potential temperature
θ_E	Equivalent potential temperature
θ_{ES}	Saturation point equivalent potential temperature
θ_{SL}	Potential temperature using T_{SL}, P_{SL}
λ	Latent heat

σ	Standard deviation
σ_u	Standard deviation of wind velocity component u
σ_v	Standard deviation of wind velocity component v
σ_w	Standard deviation of wind velocity component w
σ_y	Crosswind standard deviation of particle spread
σ_z	Vertical standard deviation of particle spread
σ_θ	Standard deviation of wind elevation fluctuation
σ_ϕ	Standard deviation of wind azimuth fluctuation
Σ	Dimensionless measure of turbulent mixing, geometric mean turbulence intensity
Σ_0	Threshold value Σ at boundary layer top
Σ_{min}	Minimum value of Σ in the profile
$\mathcal{P}$	Saturation-point pressure minus pressure of air parcel, $P_{SL} - P$

8 REFERENCES

Arya S.P.S. (1981)
Parameterizing the height of the stable atmospheric boundary layer
J. Applied Meteorology 20, pages 1192-1202

Batchelor G.K. (1967)
An Introduction to Fluid Dynamics
Cambridge University Press

Benaire M. (1980)
Determination of the dispersion coefficients from turbulence parameters
Atmospheric Planetary Boundary Layer Physics
Developments in Atmospheric Science 11, pages 261-265
edited by A. Longhetto
Elsevier

Betts A.K. (1982a)
Saturation point analysis of moist convective overturning
Journal of the Atmospheric Sciences 39 pages 1484-1505

Betts A.K. (1982b)
Cloud thermodynamic models in saturation pont coordinates
Journal of the Atmospheric Sciences 39 pages 2182-2191

Betts A.K. and Albrecht B.A. (1987)
Conserved variable analysis of the convective boundary layer Thermodynamic structure over the tropical oceans.
Journal of the Atmospheric Sciences 44 pages 83-99

Bultynck H. and Malet L.M. (1972)
Evaluation of atmospheric dilution factors for effluents diffused from an elevated continuous point source
Tellus XXIV No 5, pages 455-472

Cheung T.K. (1991)
Sodar observations of the stable lower atmospheric boundary layer at Barrow, Alaska
Boundary Layer Meteorology 57 (3) 251-274

Cieslik S., Bultynck H. and Kretzschmar J.G. (1981)
A statistical approach for estimating atmospheric stability classes from near-ground observations.
In Air Pollution Modeling and its Application Vol I pages 369-384.
De Wispelaere C. (editor) (1981) NATO CCMS Meeting 24-7 November 1980 Amsterdam

Clarke R.H. (1970)
Observational studies in the atmospheric boundary layer
Quart. J. R. Met. Soc. 96 (407) 91-114

De Maere X. and Bultynck H. (1970)
Techniques utilisees pour la mesure de la diffusion de la diffusion des effluents rejetes a l'atmosphere
Chaleur et Climats No 416, Aout 1970 pages 55-64 (stored as National Meteorological Library pamphlet p27388)

Leahey D. M. and Halitsky (1973)
Low wind turbulence statistics and related diffusion estimates from a site located in the Hudson river valley
Atmospheric Environment 7, 49-61

Derbyshire S.H. (1990)
Nieuwstadt's stable boundary layer revisited
Q. J. R. Meteorol. Soc. 116, 127-158

Enger L. (1990)
Simulation of dispersion in moderately complex terrain Part C A dispersion model for operational use.
Atmospheric Environment 24A (9) 2457-2471

Farmer S.G. (1984)
A comparison of methods of estimating stability category and boundary layer depth using routine surface observations
Special Investigations Technical Note 37
The Meteorological Office (unpublished)

Hanna S.R. Briggs G.A. Hosker R. P. (1982)
Handbook on atmospheric diffusion
US Dept of Energy Technical Information Center DOE/TIC-11223.

Hay J. S. and Pasquill F. (1959)
Diffusion from a continuous source in relation to the spectrum and scale of turbulence
Advances in Geophysics 6, 345-365

Holzworth G.C. (1972)
Mixing heights, wind speeds and potential for urban air pollution throughout the contiguous United States.
Environmental Protection Agency (Division of Meteorology)
Research Triangle Park

Holzworth G.C. (1974)
Climatological aspects of the composition and pollution of the atmosphere
World Meteororological Organisation No 393
Technical report No 139, especially pages 18-23

King J.C. (1990)
The atmospheric boundary layer over an Antarctic ice shelf
Ninth symposium on turbulence and diffusion, April 30-May3, 1990

RISO, Roskilde, Denmark. Pages 334-336

Kitaigorodskii S.A. (1988)
A note on similarity theory for atmospheric boundary layers in the presence of background stable stratification
Tellus 40A (5) 434-438

Kitaigorodskii S.A. and Joffre S.M. (1988)
In search of a simple scaling for the height of the stratified atmospheric boundary layer
Tellus 40A (5) 419-433

Koracin K. and Berkowicz R.(1988)
Nocturnal boundary layer height: Observations by acoustic sounders and predictions in terms of surface-layer parameters
Boundary Layer Meteorology 43 (1-2) 65-83

Kurzeja R.J., Berman S., and Weber A.H. (1991)
A climatological study of the nocturnal planetary boundary layer
Boundary Layer Meteorology 54 pages 105-128.

Mahrt L., Andre J.C. and Heald R.C. (1982)
On the depth of the nocturnal boundary layer
J. Applied Meteorology 21 pages 90-92

Mahrt L. et al. (1979)
An observational study of the structure of the nocturnal boundary layer
Boundary Layer Meteorology 17 pages 247-264

Maryon R.H. and Best M.J. (1993)
'NAME', 'ATMES' and the boundary layer problem
Met O (APR) Turbulence and Diffusion Note No. 204

Melas D. (1990)
Sodar estimates of surface heat flux and mixed layer depth compared with direct measurements
Atmospheric Environment 24A (11) 2847-2853

Melas D.(1991)
Using a simple resistance law to estimate friction velocity from sodar measurements
Boundary Layer Meteorology 57 (3) 275-287

Nieuwstadt F. T. M. (1984)
The turbulent structure of the stable, nocturnal boundary layer
J. Atmospheric Sciences 41 (14) 2202-2216

Parasnis S.P, Morwal S.B. (1991)
The convective boundary layer over the Deccan Plateau, India during the summer monsoon
Boundary Layer Meteorology 54 pages 59-68

Parasnis S.P, Morwal S.B. and Vernekar K.G. (1991)
Convective boundary layer in the region of the monsoon trough - a case study
Advances in Atmospheric Sciences 8 (4) 505-509

Pasquill F. (1962)
Atmospheric diffusion. The dispersion of windborne material from industrial and other sources
D Van Nostrand

Prandtl L. (1952)
Essentials of Fluid Dynamics
Blackie & Son

Stull R. B. (1988)
An introduction to boundary layer meteorology
Kluwer Academic Publishers

Wandel C. F. and Kofoed-Hansen O. R. (1962)
On the Eulerian-Lagrangian transform in the statistical theory of turbulence
J. Geophys. Res. 67, 3089

Wetzel P. J. (1982)
Towards Parameterization of the stable boundary Layer
J. Applied Meteorology 21 pages 7-13

Zilitinkevich S. S. (1972)
On the determination of the height of the Ekman boundary layer
Boundary Layer Meteorology 3, pages 141-145

9 APPENDIX 1

9.1 Notation

Equations (9) and (10) equate the spread of particles normalised by their travel distance to the component of turbulence normalised by the mean wind speed. The paper by Bultynck and Malet (1972) uses a typesetting of its equations 5,6 which is less clear to read than the equivalent equations 3,4 in De Maere and Bultynck (1970). It is therefore useful to clarify the notation.

The running mean of the fluctuation velocity squared over averaging time $T = x/(\beta\overline{u})$ is denoted by

$$\overline{v'^{\,2}_{x/(\beta_z\overline{u})}} \tag{27}$$

with dimensions L^2T^{-2}.
The combined average for sampling interval B, say 3600 seconds, is then

$$\overline{\left[v'^{\,2}_{x/(\beta_z\overline{u})}\right]}_B \tag{28}$$

with dimensions L^2T^{-2}.
Finally the square root of this average over the sampling period B is denoted by

$$\overline{\left[v'^{\,2}_{x/(\beta_z\overline{u})}\right]}^{\frac{1}{2}}_B \tag{29}$$

which has dimensions LT^{-1}.
When this is normalised by division by $\overline{u}$ the answer has no dimensions, consistent with σ_y/x or σ_z/x.

9.2 Bivane Smoothing

In a similar fashion, Leahey and Halitsky (1973) calculate plume standard deviations in the cross-wind and vertical directions by means of smoothed bivane traces. The bivane signal is smoothed over moving intervals of time $x/\beta\overline{u}$ for downwind distance x, mean wind speed $\overline{u}$, and β about 4; the results are insensitive to β and moderate departures have little effect. The standard deviation is calculated from the smoothed signal. The deviations are sampled over intervals of time for which the plume dimensions were required, then multiplied by the downwind distance.

9.3 Other Comments

The two equations (9), (10) are analogous to the equation 3.38 in Pasquill(1962) page 86-87, which is a direct result of Taylor's statistical analysis, i.e. for small time T in

which the particle has deviation X, Pasquill has

$$\overline{X^2} = \overline{u'^2}T^2 \tag{30}$$

by applying the usual rules of differention to the mean values of fluctuating variables and their products. Taking square roots

$$\sigma_X = \sqrt{\overline{u'^2}}T \tag{31}$$

and using $T = x/(\overline{u})$ leads to

$$\sigma_X/x = \sqrt{\overline{u'^2}}/\overline{u} \tag{32}$$

The similarity to the dimensionless measure of the turbulence intensity (which has long been in use: see for example Stull (1988) page 43) is also evident:

$$I = \sigma_M/\overline{M} \tag{33}$$

where I is the turbulence intensity, σ_M is the standard deviation of the wind speed M and the mean wind speed is $\overline{M}$.

10 APPENDIX 2. PROFILES FROM MODEL AND RADIOSONDE

A small sample of the many possible profiles are included in this report. Each page refers to radiosonde measurements or to 'NAME' model profiles (the latter from the forecast suite) and are labelled accordingly. The date and time are given. Positions are identified by the name of the relevant radiosonde station. The grid point is for the Limited Area Grid and some points are just off the coast from the adjacent radiosonde station. Since these stations are all within 5 degrees of the Greenwich meridian, the profiles can be regarded as being at the same solar time.

Each figure contains four profiles, with height calculated from the hydrostatic equation (applied to each layer in turn). The four profiles are as below:

1. Dew point and temperature
2. Wind-speed
3. Potential temperature calculated from the pressure and temperature data used to plot profile 1.
4. The value of the empirical Sigma parameter Σ. Equations 12, 16-23 were used to estimate Σ as a function of height from the values of potential temperature and wind-speed interpolated at each step. A broken line is drawn at the height where Σ crosses the threshold Σ_0 and indicates the boundary layer depth as diagnosed by the empirical Sigma method. This height should be compared with the profiles 1, 2 and 3.

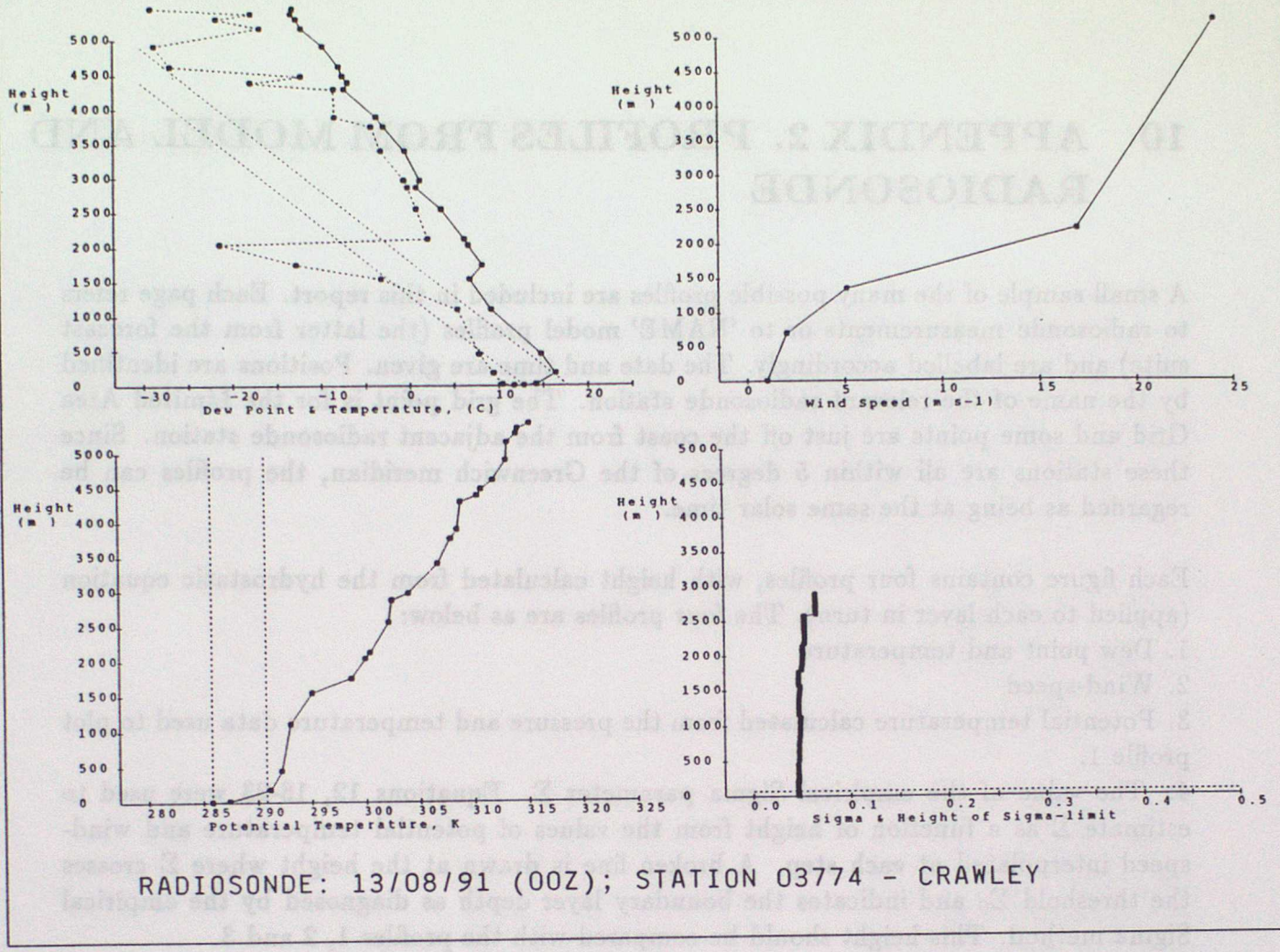

RADIOSONDE: 13/08/91 (00Z); STATION 03774 - CRAWLEY

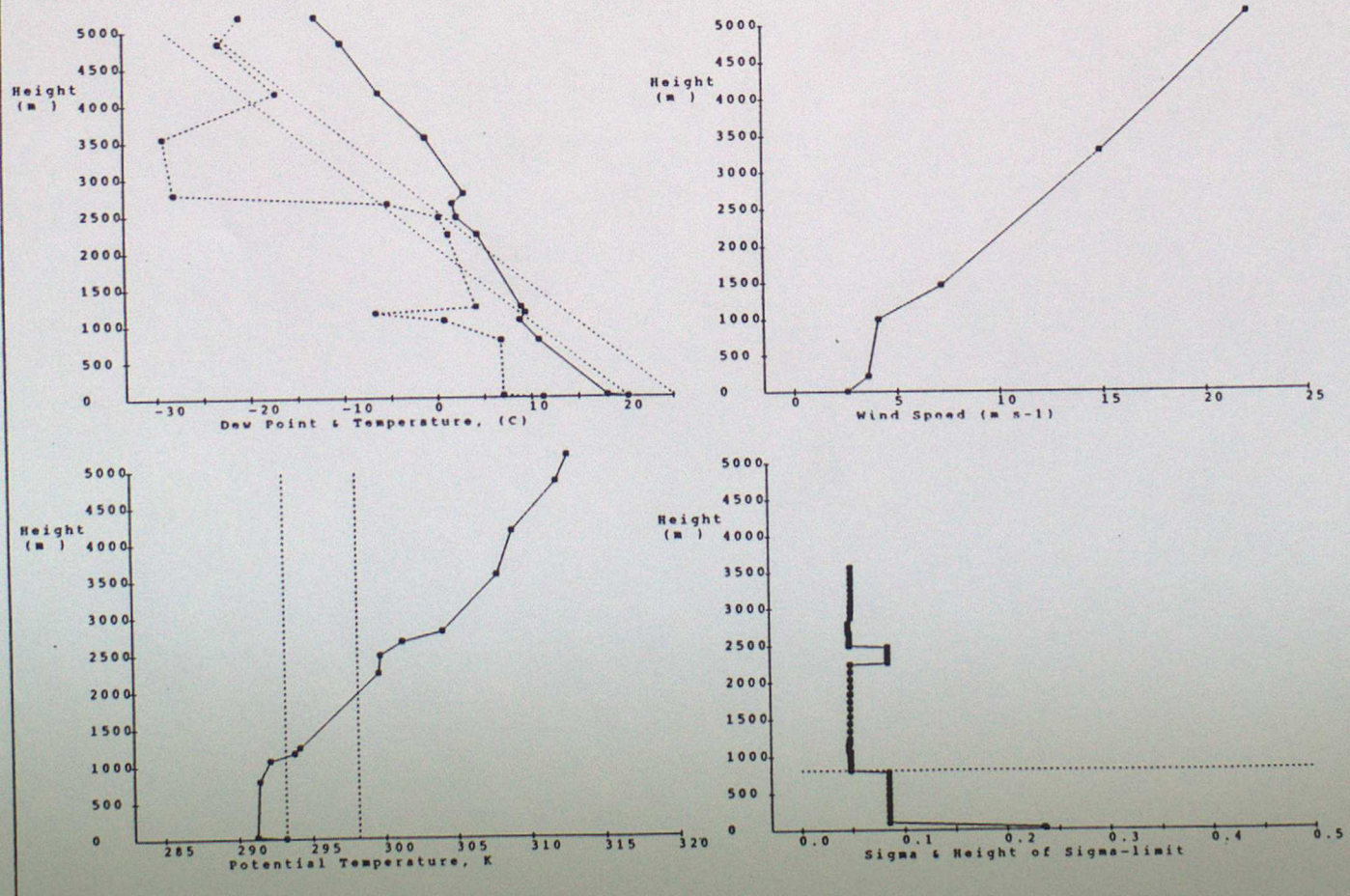

RADIOSONDE: 13/08/91 (12Z); STATION 03774 - CRAWLEY

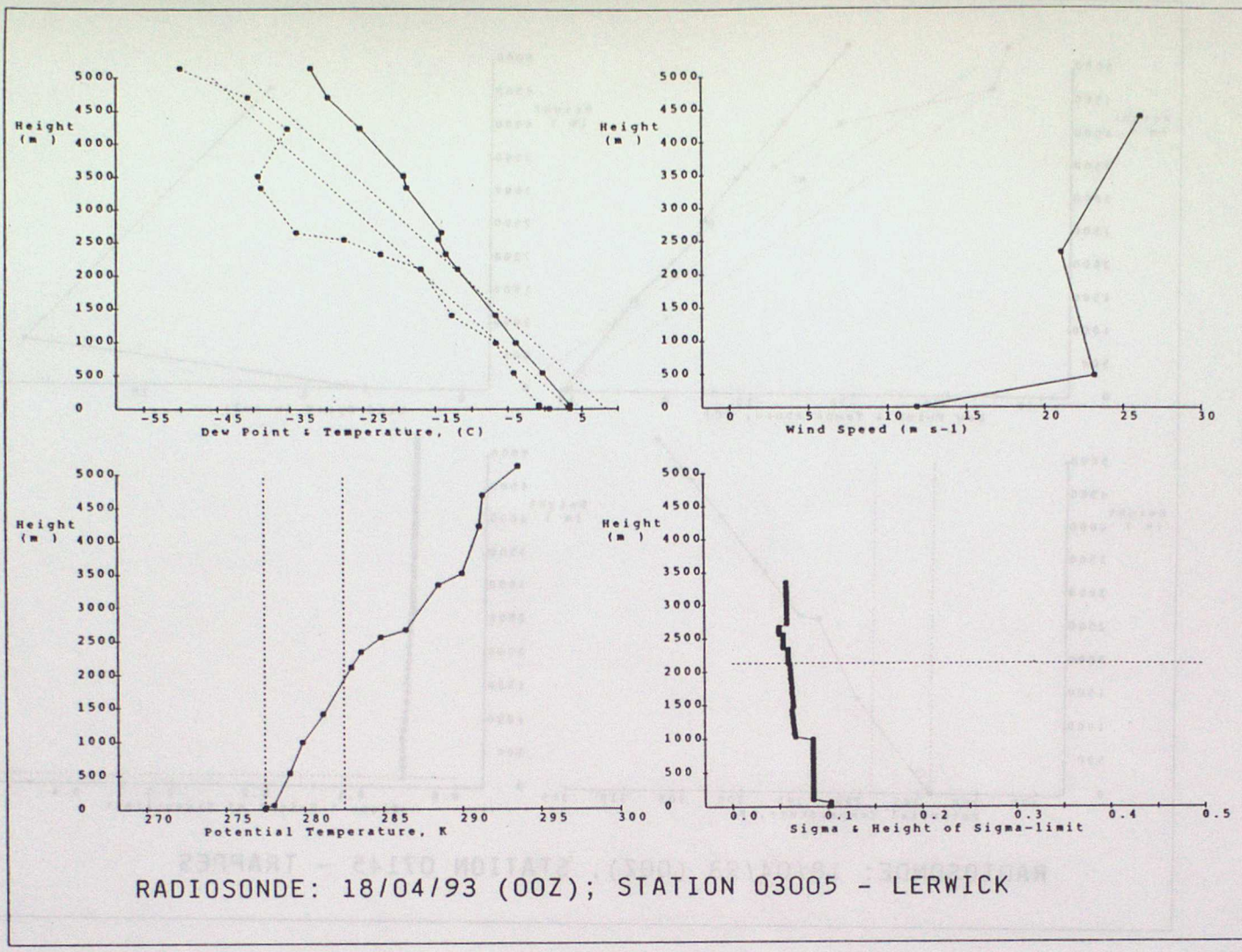

RADIOSONDE: 18/04/93 (00Z); STATION 03005 - LERWICK

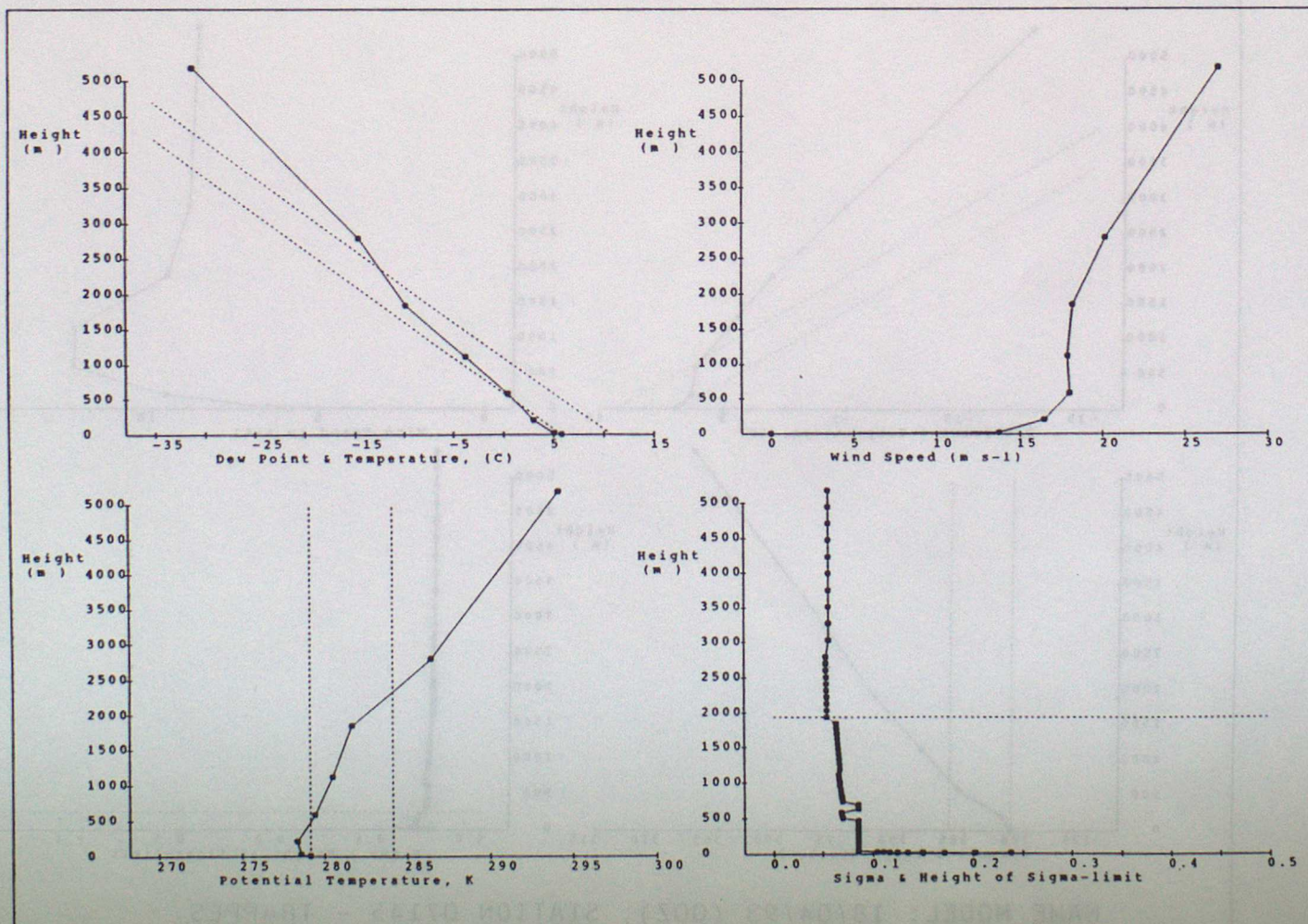

NAME MODEL: 18/04/93 (00Z); STATION 03005 - LERWICK

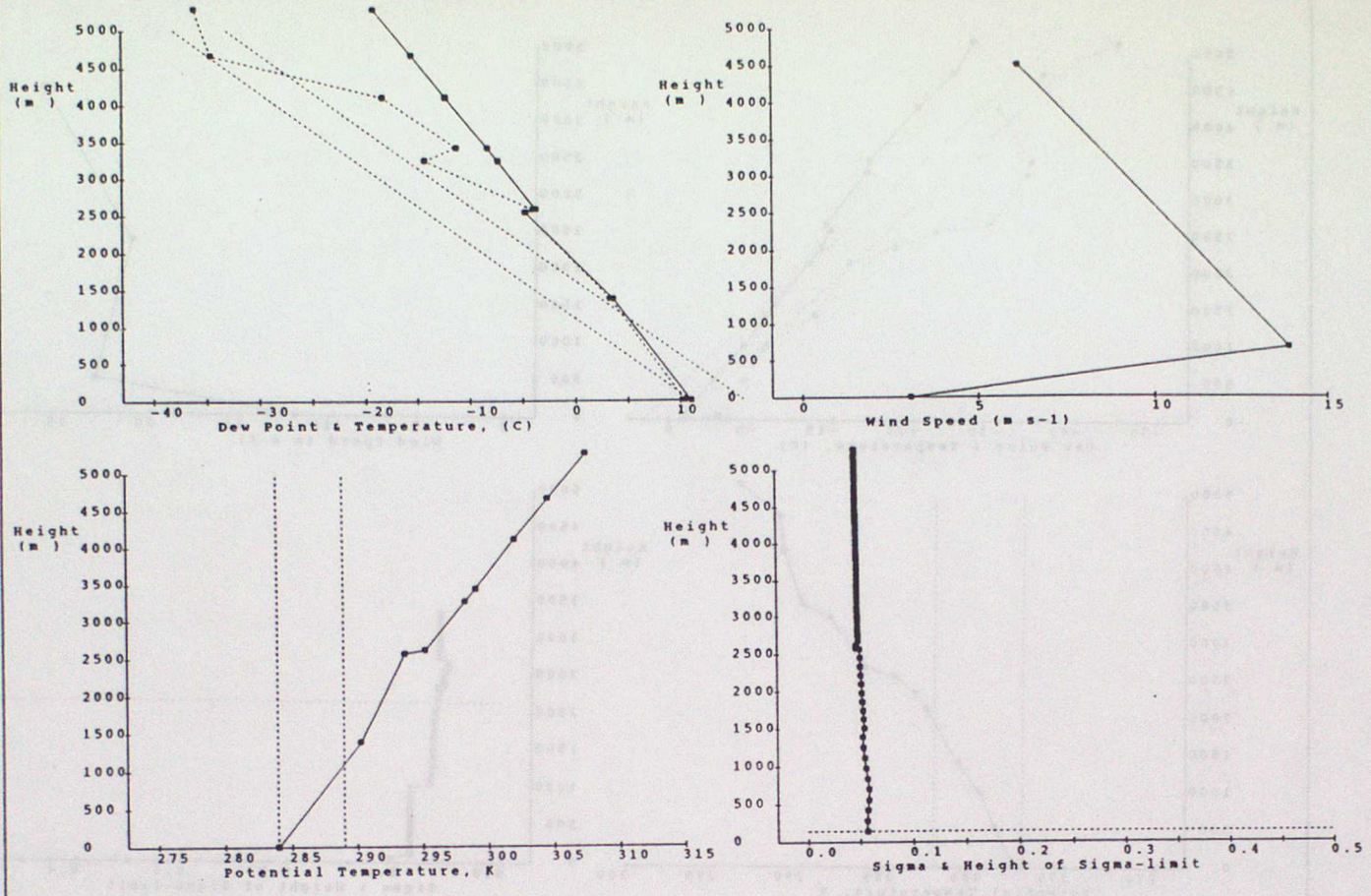

RADIOSONDE: 18/04/93 (00Z); STATION 07145 - TRAPPES

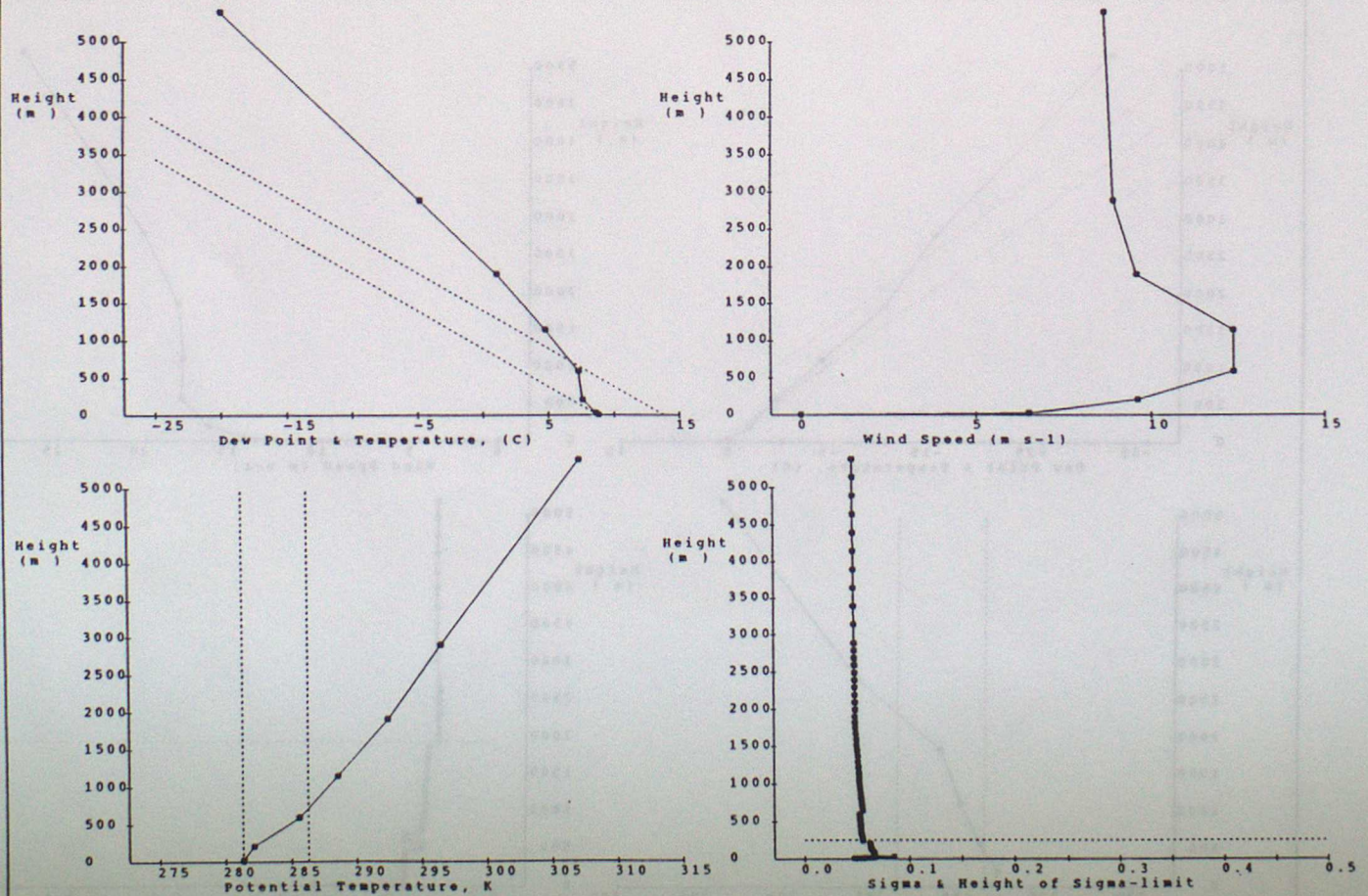

NAME MODEL: 18/04/93 (00Z); STATION 07145 - TRAPPES

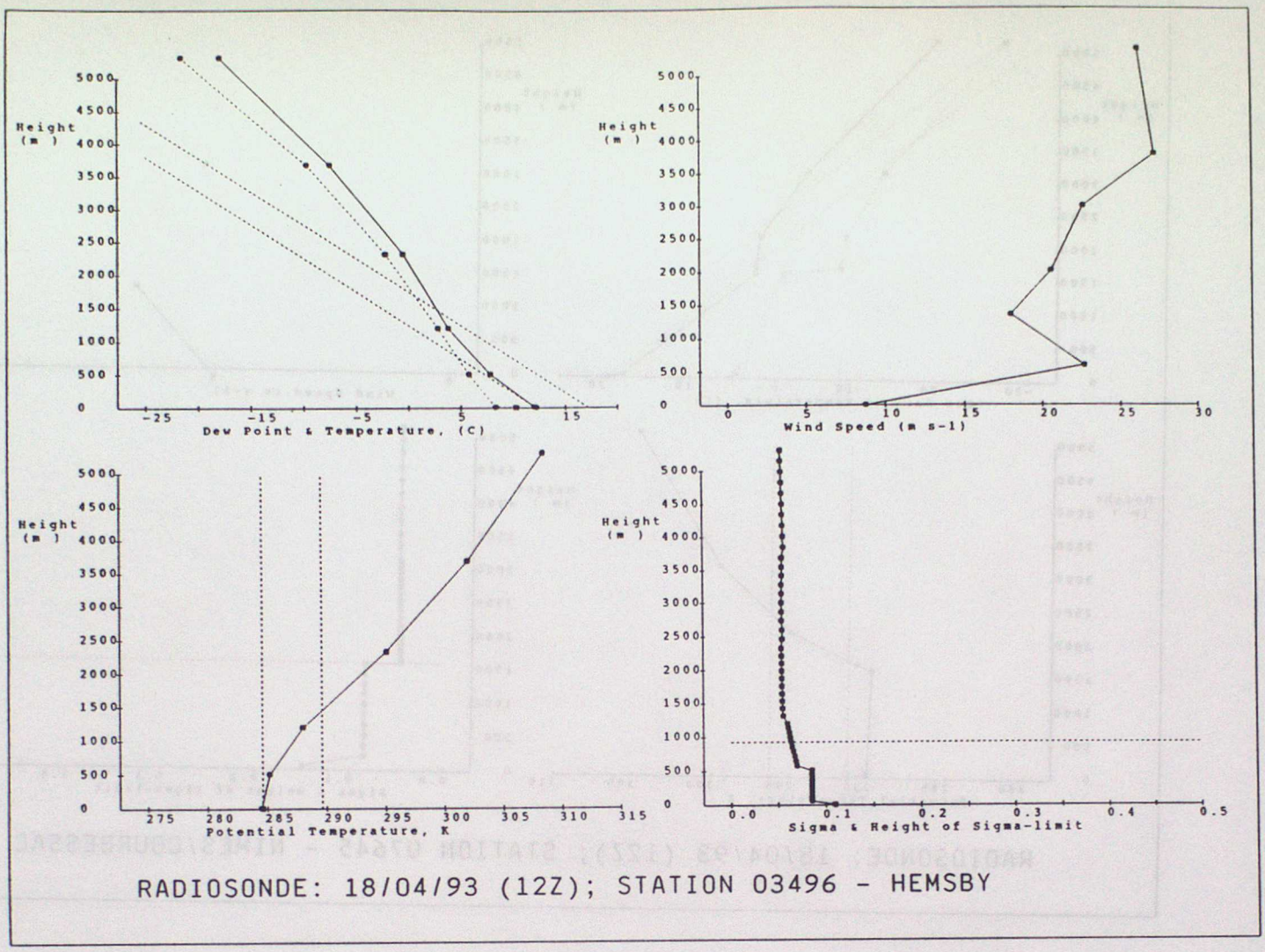

RADIOSONDE: 18/04/93 (12Z); STATION 03496 - HEMSBY

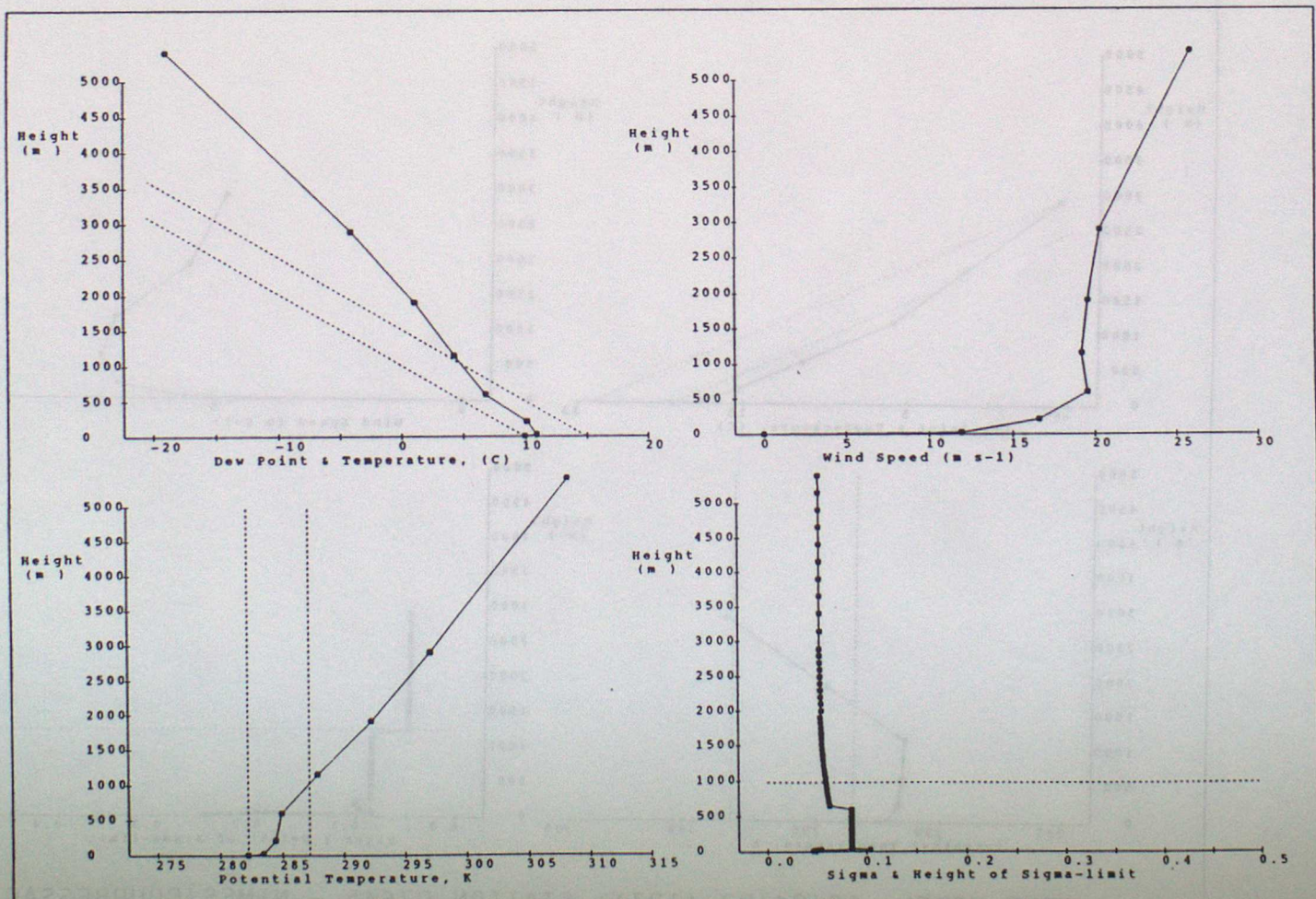

NAME MODEL: 18/04/93 (12Z); STATION 03496 - HEMSBY

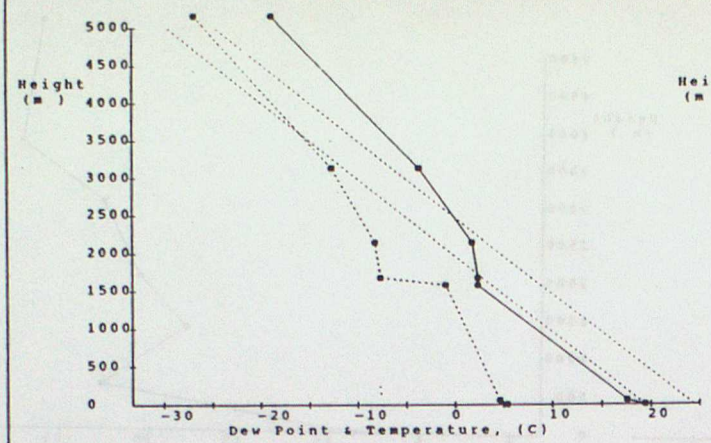

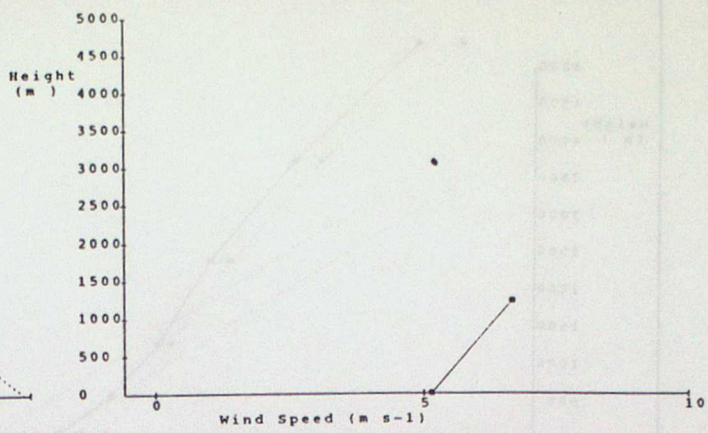

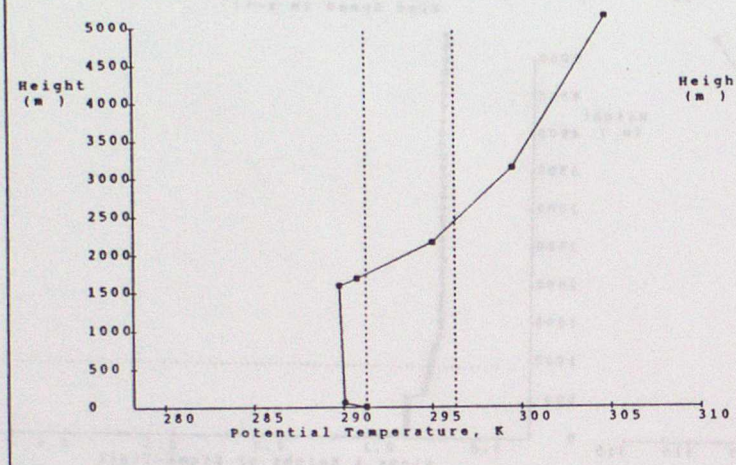

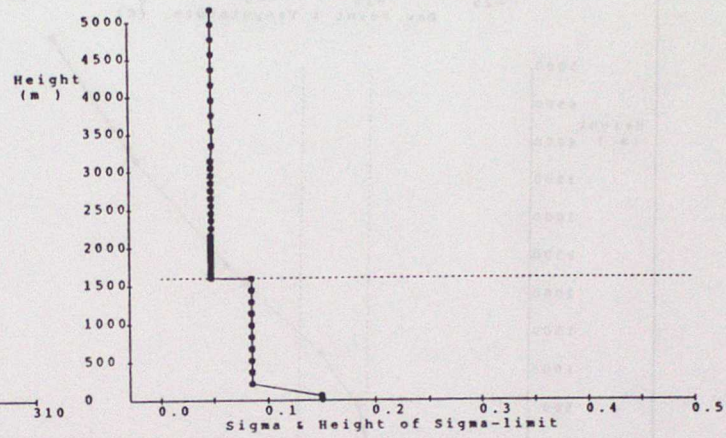

RADIOSONDE: 18/04/93 (12Z); STATION 07645 - NIMES/COURBESSAC

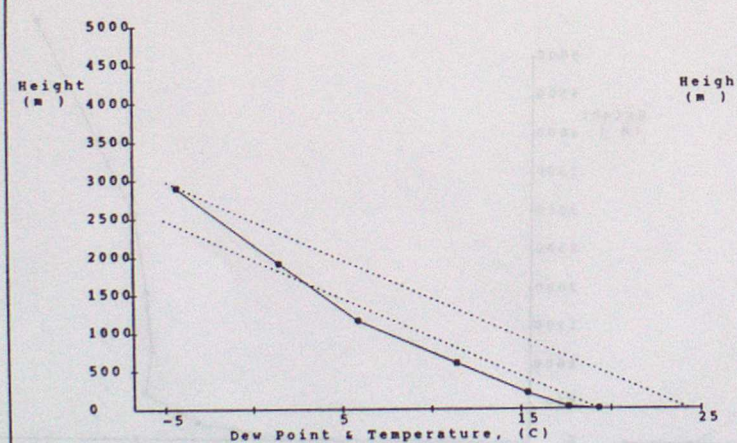

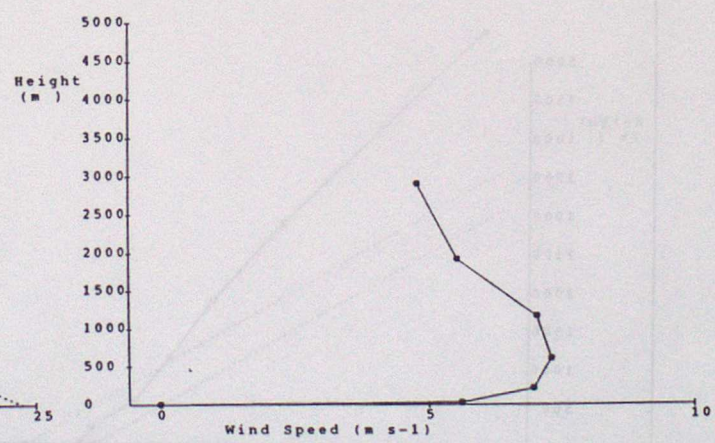

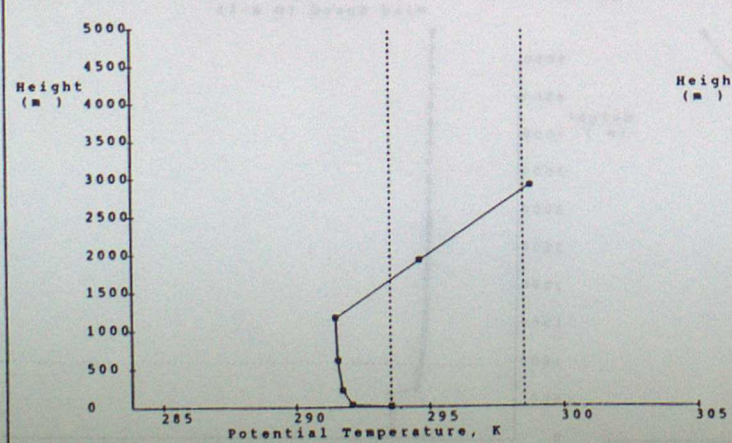

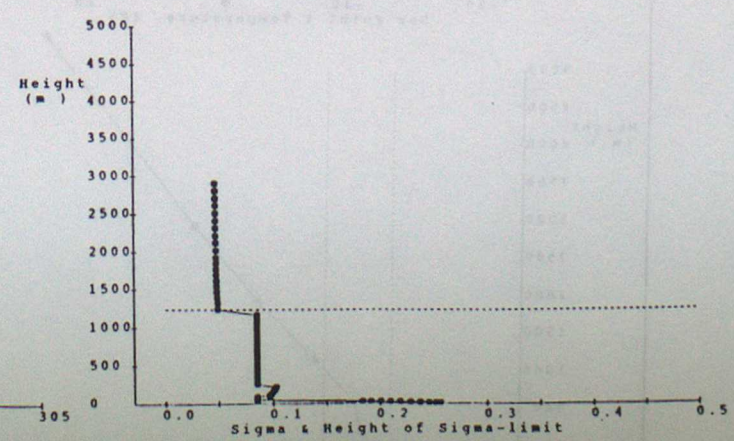

NAME MODEL: 18/04/93 (12Z); STATION 07645 - NIMES/COURBESSAC